Israel Journal of Chemistry

IJC

Official Journal of the Israel Chemical Society

REPRINT

www.ijc.wiley-vch.de

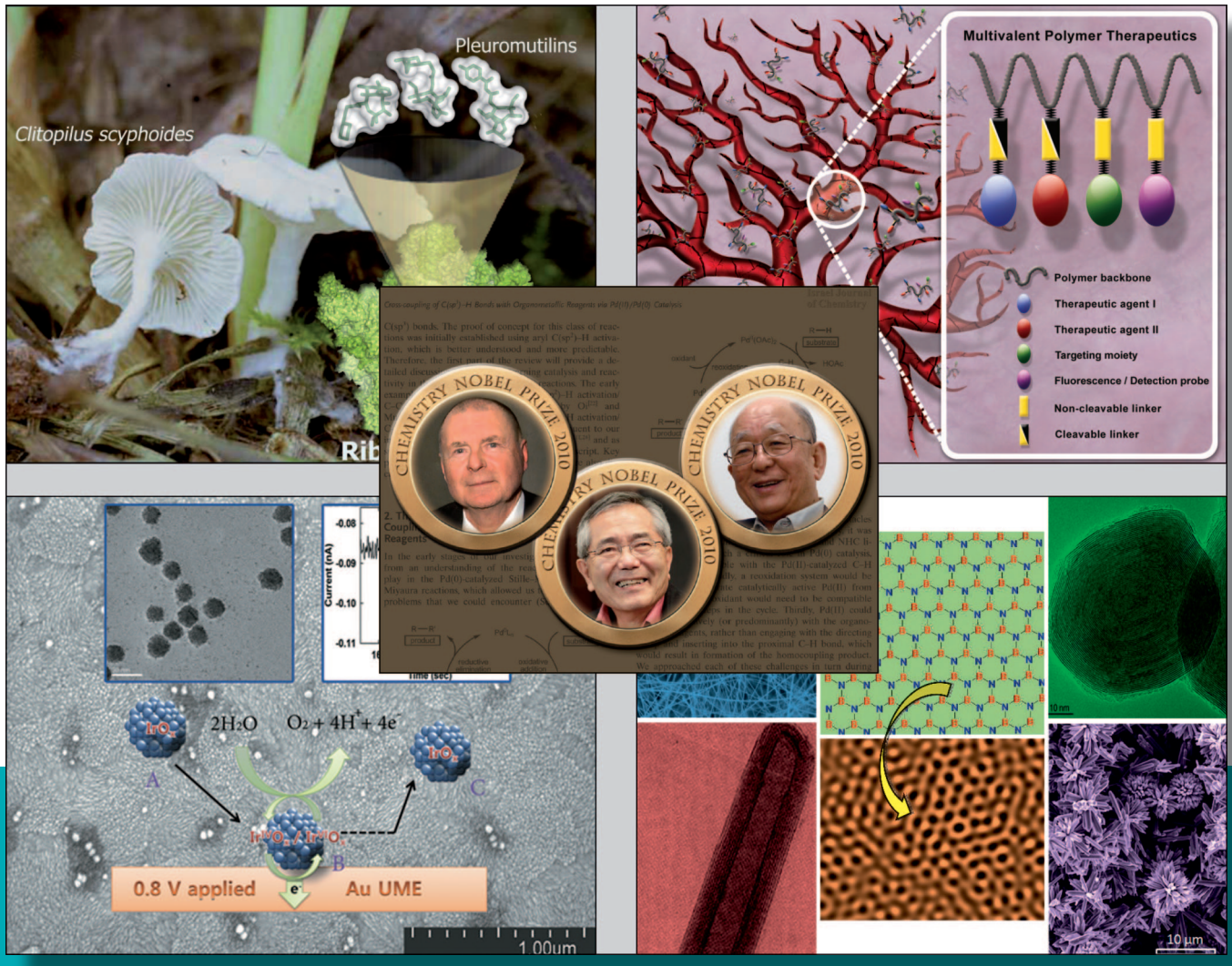

WILEY-VCH

Communication

Israel Journal of Chemistry

DOI: 10.1002/ijch.201800068

Novel Topology in Semiconducting Tetrathiafulvalene Lanthanide Metal-Organic Frameworks

Lilia S. Xie[a] and Mircea Dincă*[a]

Dedicated to Professor Omar M. Yaghi on the occasion of his receipt of the 2018 Wolf Prize

Abstract: Tetrathiafulvalene tetrabenzoate (TTFTB) and several lanthanide ions self-assemble into metal-organic frameworks (MOFs) that exhibit a novel topology, a (3,3,3,6,6)-coordinated net, which features an unusual ligand coordination mode and stacking motif. The Yb and Lu MOFs are electrically conductive, with pellet conductivity values of 9(7) $\times$ 10^{-7} and 3(2) $\times$ 10^{-7} S/cm, respectively. The crystallographically-determined bond lengths indicate partial oxidation of the ligand, with close S···S contacts between ligands providing likely charge transport pathways in the material. Magnetometry reveals temperature-independent paramagnetism, consistent with the presence of ligand-based radicals, as well as weak antiferromagnetic coupling between Yb^{3+} centers. These results illustrate the diversity of MOF structures and properties that are accessible with the TTFTB ligand owing to its electroactive nature, propensity for intermolecular interactions, and conformational flexibility.

Keywords: metal–organic frameworks · lanthanides · structure elucidation · π interactions · tetrathiafulvalene

The advent of reticular chemistry and its application to metal–organic frameworks (MOFs) has brought about the rapid discovery of thousands of new structures[1] and their application in numerous areas.[2–5] Whereas the assembly of most MOFs is driven by the formation of inorganic secondary building units (SBUs), our group has recently shown that the organic ligands can also direct structure through the formation of supramolecular π interactions that define an organic SBU, as demonstrated with the isolation of an unprecedented topology in MIT-25.[6] The latter is based on the tetrathiafulvalene tetrabenzoate (TTFTB) linker, which forms MOFs with diverse topologies, all of which exhibit strong π interactions.[7–10] In addition to their structure-defining roles, these interactions lead to several desirable physical properties, including electrical[7] and proton conductivity,[8] and redox-switchable breathing behavior.[9] We hypothesized that TTFTB frameworks based on lanthanides might exhibit new topologies and physical properties due to the varied coordination geometries of the lanthanides coupled with the electroactive and flexible nature of this ligand. Herein, we report the structural characterization along with the electrical and magnetic properties of the TTFTB MOFs with Tm^{3+}, Yb^{3+}, and Lu^{3+}.

Reaction of $Tm(NO_3)_3 \cdot 5H_2O$ with H_4TTFTB in a mixture of *N,N*-dimethylformamide (DMF), water, and ethanol yielded red plate-shaped crystals of $Tm_6H_2(TTFTB)_5(DMF)_4(H_2O)_8$ ($Tm_6(TTFTB)_5$) (Table S1). Single crystal X-ray diffraction studies showed that the inorganic SBUs of the resulting MOF comprise two Tm atoms coordinated by carboxylates from six ligands, in addition to DMF and water (Figure 1a and b). The TTFTB ligands connect these SBUs in two-dimensional layers. Two of the three crystallographically-independent ligands are bonded to four separate SBUs, the typical coordination mode for a tetratopic ligand.[11] The third type of ligand bridges two SBUs through diagonal benzoate groups, with the TTF core approximately orthogonal to the other two.

Figure 2 illustrates the idealized connectivity of one layer of $Tm_6(TTFTB)_5$, with the three types of ligands labeled. Both the TTF1 and TTF2 ligands can be considered as two linked three-connected nodes. Because TTF3 bridges only two SBUs, it is appropriately described by a single edge.

The result is a (3,3,3,6,6)-coordinated net, with the point symbol $(4.6^2)_2(4^2.6)_4(4^6.6^4.8^5)(4^6.6^6.8^3)_2$. To the best of our knowledge, the structure of $Tm_6(TTFTB)_5$ constitutes a novel topology, which we hereby call ***lsx***.[12,13]

In the bulk structure of $Tm_6(TTFTB)_5$, five TTF cores from three different layers pack in close proximity (Figure 3a). Each group of five TTFs consists of two sets of dimers (TTF1 and TTF2) and an orthogonal TTF (TTF3). Though this arrangement contrasts with the parallel π-stacking modes of other TTFTB MOFs,[6–10] it is somewhat reminiscent of the κ packing arrangement, consisting of orthogonal TTF dimers, found in many organic metals and superconductors.[14,15] Close S···S contacts as short as 3.72 Å are present between all S atoms within the dimers in $Tm_6(TTFTB)_5$. In addition, TTF1 and TTF3 exhibit relatively close S···S distances of 4.04 Å and 4.41 Å. The central C–C and C–S bond lengths in all three

[a] L. S. Xie, Prof. M. Dincă
Department of Chemistry
Massachusetts Institute of Technology
77 Massachusetts Avenue, Cambridge, MA 02139 (USA)
E-mail: mdinca@mit.edu

Supporting information for this article is available on the WWW under https://doi.org/10.1002/ijch.201800068

Israel Journal of Chemistry

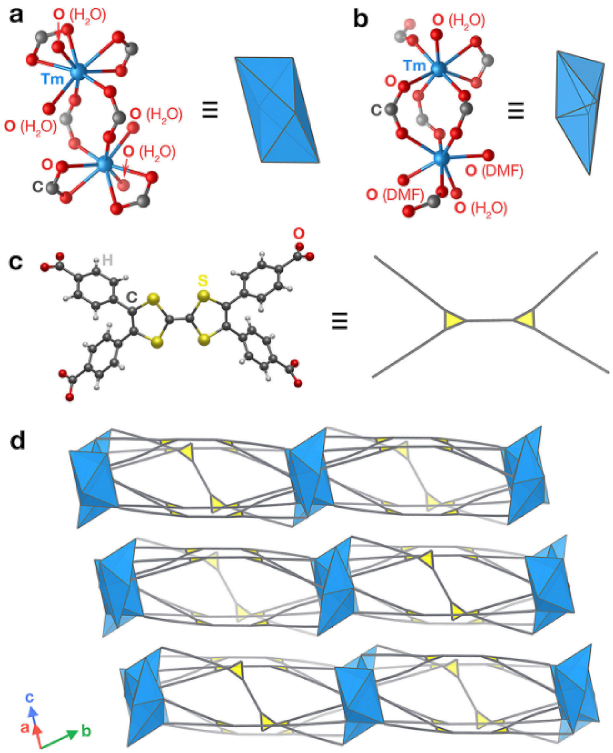

Figure 1. a) and b) Coordination environment and structural representation of secondary building units in $Tm_6(TTFTB)_5$. c) Structure and representation of TTFTB ligand. d) View of the structure of $Tm_6(TTFTB)_5$ showing the stacking of two-dimensional layers.

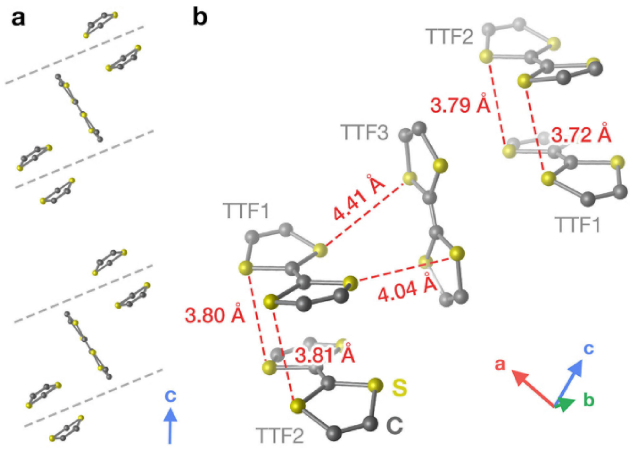

Figure 3. a) Packing arrangement of TTF units in $Tm_6(TTFTB)_5$; gray dotted lines indicate boundaries between covalently bonded layers. b) Intermolecular S···S distances between adjacent ligands of a TTF pentamer.

ligands (Table S2) are similar to those in electrically conductive TTFTB MOFs with partially oxidized ligands.[7] These parameters suggest that electronic delocalization of free charge carriers is possible in this structure.

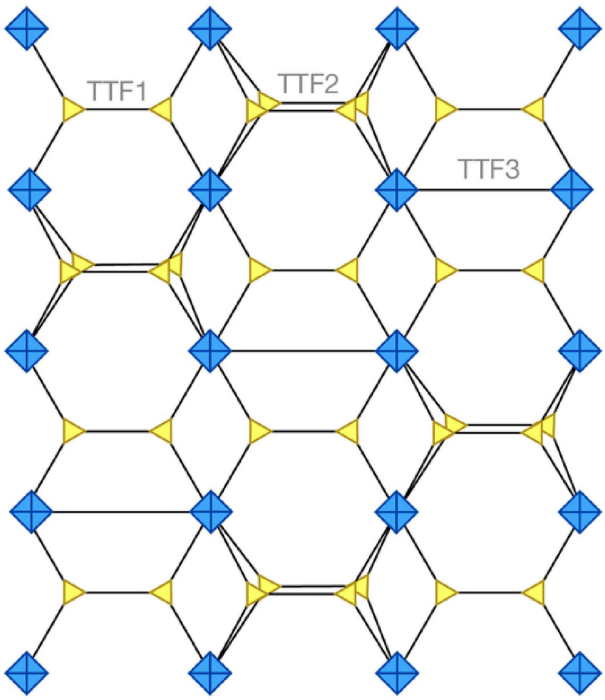

Figure 2. Idealized connectivity of a single layer of $Tm_6(TTFTB)_5$ with crystallographically independent ligands labeled. Three-connected nodes are indicated by yellow triangles, and six-connected nodes by blue octahedra.

Samples of $Tm_6(TTFTB)_5$ exhibited concomitant polymorphism with an unidentified phase, which precluded bulk characterization of the desired structure in this system. In contrast, powder X-ray diffraction (PXRD) of the Yb and Lu analogues confirmed them to be phase-pure and isostructural to $Tm_6(TTFTB)_5$ (Figure 4a). Thermogravimetric analysis of $Yb_6(TTFTB)_5$ and $Lu_6(TTFTB)_5$ revealed stability up to 300 °C (Figure S2). A nitrogen adsorption isotherm of $Yb_6(TTFTB)_5$ after activation at 220 °C (Figure S3) yielded a Brunauer–Emmett–Teller surface area of 400(1) $cm^2 g^{-1}$, confirming its microporous nature (under these conditions, $Lu_6(TTFTB)_5$ exhibited a surface area of only 70 $cm^2 g^{-1}$, indicating different stabilities despite their structural similarities).

To investigate the electrical conductivities of $Yb_6(TTFTB)_5$ and $Lu_6(TTFTB)_5$, we measured a total of 8 two-contact probe pressed pellet devices from 3 separate batches of each material. Average conductivities of $9(7)\times10^{-7}$ and $3(2)\times10^{-7}$ S cm^{-1} were obtained for $Yb_6(TTFTB)_5$ and $Lu_6(TTFTB)_5$, respectively, with champion conductivities of 2.6×10^{-6} and 7.5×10^{-7} S cm^{-1} (Figures 4b and S4). These values are similar to the pellet conductivities of other TTFTB MOFs.[16] We note that single crystal studies may yet reveal higher conductivities due to the elimination of grain boundaries and the anisotropic nature of the TTF stacking.

Magnetometry measurements on powder samples of $Yb_6(TTFTB)_5$ and $Lu_6(TTFTB)_5$ revealed paramagnetic behavior

Israel Journal of Chemistry

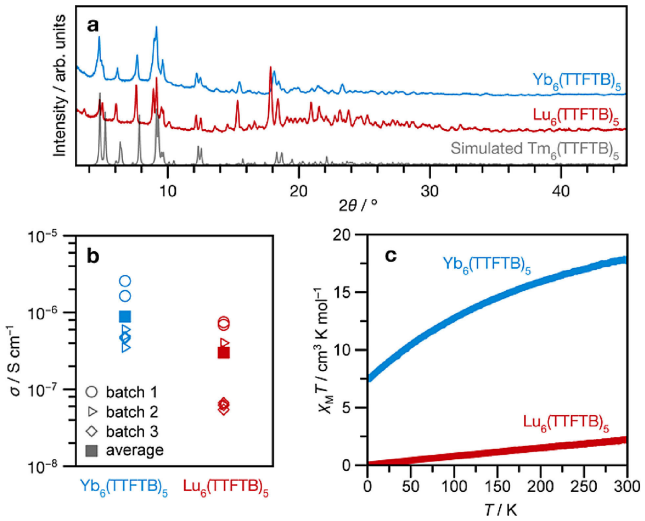

Figure 4. a) Experimental powder X-ray diffraction patterns for $Yb_6(TTFTB)_5$ and $Lu_6(TTFTB)_5$ compared to the simulated pattern from the single crystal structure of $Tm_6(TTFTB)_5$. b) Two-contact probe pressed pellet conductivities of $Yb_6(TTFTB)_5$ and $Lu_6(TTFTB)_5$. c) Magnetic susceptibility data for $Yb_6(TTFTB)_5$ and $Lu_6(TTFTB)_5$ taken under an applied dc field of 1000 Oe.

down to 2.0 K (Figure 4c). Temperature-independent paramagnetism (TIP) is observed for both MOFs, with a magnitude of about 7.4×10^{-3} $cm^3\,mol^{-1}$ in $Lu_6(TTFTB)_5$. We attribute this behavior to spin contributions from partially delocalized charge carriers on the TTFTB ligands.[17–19] Similarly, the total susceptibility of the Yb MOF can be considered as the sum of the paramagnetic component from the Yb centers (χ_P) and a TIP contribution from ligand spins (χ_{TIP}). Taking the susceptibility of $Lu_6(TTFTB)_5$ as a good estimate for χ_{TIP} in the Yb compound, we obtain a value for $\chi_P T$ at 300 K of 15.6 cm^3 K mol^{-1} in the latter, very close to the theoretical value for 6 magnetically isolated Yb^{3+} ions of 15.4 $cm^3\,K\,mol^{-1}$. With decreasing temperature, the value of $\chi_P T$ decreases monotonically to 7.4 $cm^3\,K\,mol^{-1}$ at 2.0 K. Fitting the susceptibility data between 100 and 300 K to the Curie–Weiss law $\chi = C/(T-\theta)$ yields values for the Curie constant, C, and Curie temperature, θ, of 18.7 $cm^3\,K\,mol^{-1}$ and −59.2 K, respectively (Figure S5). The decrease in $\chi_P T$ at lower temperatures and the negative value of θ suggest weak antiferromagnetic interactions between adjacent Yb^{3+} ions.

In conclusion, we have shown that Tm^{3+}, Yb^{3+}, and Lu^{3+} react with H_4TTFTB to form MOFs exhibiting a new topology. These structures are likely influenced by a unique TTF packing motif and ligand coordination mode. The Yb and Lu MOFs are electrically conductive, and TIP in these materials suggests partial oxidation of the ligands, consistent with the presence of free charge carriers. These findings add to the structural diversity of MOFs based on the TTFTB ligand, illustrating that the redox-active nature and π interactions of this unique linker give rise to new modes of self-assembly.

Acknowledgments

This work was supported by the U.S. Department of Energy, Office of Science, Office of Basic Energy Sciences (DE-SC0018235). L.S.X. thanks the National Science Foundation for support through the Graduate Research Fellowship Program (1122374). We gratefully acknowledge Dr. Peter Müller, Dr. Jonathan Becker, Wesley Transue, and Dr. Charlene Tsay for assistance with crystallography.

References

[1] a) M. Eddaoudi, J. Kim, N. Rosi, D. Vodak, J. Wachter, M. O'Keeffe, O. M. Yaghi, *Science* **2002**, *295*, 469–472; b) O. M. Yaghi, M. O'Keeffe, N. W. Ockwig, H. K. Chae, M. Eddaoudi, J. Kim, *Nature* **2003**, *423*, 705–714; c) F. Nouar, J. F. Eubank, T. Bousquet, L. Wojtas, M. J. Zaworotko, M. Eddaoudi, *J. Am. Chem. Soc.* **2008**, *130*, 1833–1835; d) D. J. Tranchemontagne, J. L. Mendoza-Cortés, M. O'Keeffe, O. M. Yaghi, *Chem. Soc. Rev.* **2009**, *38*, 1257–1283; e) T. R. Cook, Y.-R. Zheng, P. J. Stang, *Chem. Rev.* **2013**, *113*, 734–777; f) W. Lu, Z. Wei, Z.-Y. Gu, T.-F. Liu, J. Park, J. Park, J. Tian, M. Zhang, Q. Zhang, T. Gentle III, M. Bosch, H.-C. Zhou, *Chem. Soc. Rev.* **2014**, *43*, 5561–5593.

[2] L. J. Murray, M. Dincă, J. R. Long, *Chem. Soc. Rev.* **2009**, *38*, 1294–1314.

[3] J. Lee, O. K. Farha, J. Roberts, K. A. Scheidt, S. T. Nguyen, J. T. Hupp, *Chem. Soc. Rev.* **2009**, *38*, 1450–1459.

[4] J.-R. Li, J. Sculley, H.-C. Zhou, *Chem. Rev.* **2012**, *112*, 869–932.

[5] L. E. Kreno, K. Leong, O. K. Farha, M. Allendorf, R. P. Van Duyne, J. T. Hupp, *Chem. Rev.* **2012**, *112*, 1105–1125.

[6] S. S. Park, C. H. Hendon, A. J. Fielding, A. Walsh, M. O'Keeffe, M. Dincă, *J. Am. Chem. Soc.* **2017**, *139*, 3619–3622.

[7] a) T. C. Narayan, T. Miyakai, S. Seki, M. Dincă, *J. Am. Chem. Soc.* **2012**, *134*, 12932–12935; b) S. S. Park, E. R. Hontz, L. Sun, C. H. Hendon, A. Walsh, T. Van Voorhis, M. Dincă, *J. Am. Chem. Soc.* **2015**, *137*, 1774–1777.

[8] S. S. Park, A. J. Rieth, C. H. Hendon, M. Dincă, *J. Am. Chem. Soc.* **2018**, *140*, 2016–2019.

[9] J. Su, S. Yuan, H.-Y. Wang, L. Huang, J.-Y. Ge, E. Joseph, J. Qin, T. Cagin, J.-L. Zuo, H.-C. Zhou, *Nat. Commun.* **2017**, *8*, 2008.

[10] B. Chen, Z.-P. Lv, C. F. Leong, Y. Zhao, D. M. D'Alessandro, J.-L. Zuo, *Cryst. Growth Des.* **2015**, *15*, 1861–1870.

[11] a) M. O'Keeffe, O. M. Yaghi, *Chem. Rev.* **2012**, *112*, 675–702; b) M. Li, D. Li, M. O'Keeffe, O. M. Yaghi, *Chem. Rev.* **2014**, *114*, 1343–1370.

[12] M. O'Keeffe, M. A. Peskov, S. J. Ramsden, O. M. Yaghi, *Acc. Chem. Res.* **2008**, *41*, 1782–1789.

[13] V. A. Blatov, A. P. Shevchenko, D. M. Proserpio, *Cryst. Growth Des.* **2014**, *14*, 3576–3586.

[14] a) H. Urayama, H. Yamochi, G. Saito, K. Nozawa, T. Sugano, M. Kinoshita, S. Sato, K. Oshima, A. Kawamoto, J. Tanaka, *Chem. Lett.* **1988**, *17*, 55–58; b) A. M. Kini, U. Geiser, H. H. Wang, K. D. Carlson, J. M. Williams, W. K. Kwok, K. G. Vandervoort, J. E. Thompson, D. L. Stupka, D. Jung, M.-H. Whangbo, *Inorg. Chem.* **1990**, *29*, 2555–2557; c) J. M. Williams, A. M. Kini, H. H. Wang, K. D. Carlson, U. Geiser, L. K. Montgomery, G. J. Pyrka, D. M. Watkins, J. M. Kommers, S. J. Boryschuk, A. V. S. Crouch, W. K. Kwok, J. E. Schirber, D. L. Overmyer, D. Jung, M.-H. Whangbo, *Inorg. Chem.* **1990**, 3272–3274.

[15] M. R. Bryce, *Chem. Soc. Rev.* **1991**, *20*, 355–390.
[16] L. Sun, S. S. Park, D. Sheberla, M. Dincă, *J. Am. Chem. Soc.* **2016**, *138*, 14772–14782.
[17] R. G. Kepler, *J. Chem. Phys.* **1963**, *39*, 3528–3532.
[18] M. Clemente-León, E. Coronado, J. R. Galán-Mascarós, C. Giménez-Saiz, C. J. Gómez-García, E. Ribera, J. Vidal-Gancedo, C. Rovira, E. Canadell, V. Laukhin, *Inorg. Chem.* **2001**, *40*, 3526–3533.
[19] F. J. Rizzuto, C. Hua, B. Chan, T. B. Faust, A. Rawal, C. F. Leong, J. M. Hook, C. J. Kepert, D. M. D'Alessandro, *Phys. Chem. Chem. Phys.* **2015**, *17*, 11252–11259.

Received: June 13, 2018
Accepted: July 16, 2018
Published online on August 9, 2018